View Article Online
View Journal | View Issue

Open Access Article. Published on 30 juin 2025. Downloaded on 11/04/2026 17:44:27.
This article is licensed under a Creative Commons Attribution 3.0 Unported Licence.

Faraday Discussions

Volume: 263

Frontiers in Physical Chemistry for Lignin Valorisation

ROYAL SOCIETY OF CHEMISTRY

Faraday Discussions
Cite this: *Faraday Discuss.*, 2026, **263**, 445

PAPER

Tuning ester derivatives of organosolv *vs.* technical lignin for improved thermoplastic materials†

Mahendra Kothottil Mohan, ‡[a] T. Tran Ho, ‡[a] Carmen Köster,[a] Oliver Järvik,[b] Maria Kulp[a] and Yevgen Karpichev *[a]

Received 4th May 2025, Accepted 30th June 2025
DOI: 10.1039/d5fd00068h

In this study, lignin from two different sources – organosolv pine and hydrolysis birch – were chemically modified through esterification of hydroxyl groups using octanoyl (C8), lauroyl (C12), and palmitoyl (C16) chlorides, as well as through chloromethylation followed by esterification with tetradecanoic acid (C14) and benzoic acid. Modification of lignin was confirmed by FTIR and NMR spectroscopy. The esterified lignin samples were loaded into polylactic acid (PLA) at loadings of 10%, 20%, and 30% using a solvent casting method. Thermal and mechanical properties of PLA/lignin composites revealed that esterification significantly affected the polymer matrix properties. PLA could sustain as much as 30% lignin ester loading without affecting the film integrity. Among the variations, hydrolysis lignin ester (HLE) and benzoic acid ester (BAEP) enhanced the heat stability of PLA, while esterification with palmitoyl chloride (OHLE_C16) increased its elasticity through plasticization.

Open Access Article. Published on 30 juin 2025. Downloaded on 11/04/2026 17:44:27.
This article is licensed under a Creative Commons Attribution 3.0 Unported Licence.

1. Introduction

Despite its abundance (up to 35%) and aromatic-rich structure, lignin receives much less attention in biorefineries compared to sugar derivatives in lignocellulosic biomass.[1,2] For instance, the downstream process primarily utilizes black liquor, which contains mostly lignin, for electricity production, a common scenario for every pulp and paper industry worldwide.[3] The difficulties arise in lignin's valorisation due to its heterogeneity of structure and properties that drastically change depending on the botanical origin, as well as the severity of the fractionation process. Lignin's chemistry significantly varies in the compositions of the three main monolignols, *p*-hydroxyphenyl (H), guaiacyl (G), and syringyl (S) (Fig. 1).[4] As

[a]*Department of Chemistry and Biotechnology, Tallinn University of Technology (TalTech), Akadeemia tee 15, 12618 Tallinn, Estonia. E-mail: yevgen.karpichev@taltech.ee; Fax: +372 620 2994; Tel: +372 620 4381*
[b]*Department of Energy Technology, Tallinn University of Technology (TalTech), Ehitajate tee 5, 19086 Tallinn, Estonia*

† Electronic supplementary information (ESI) available. See DOI: https://doi.org/10.1039/d5fd00068h
‡ These authors contributed equally to the publication.

Open Access Article. Published on 30 juin 2025. Downloaded on 11/04/2026 17:44:27.
This article is licensed under a Creative Commons Attribution 3.0 Unported Licence.

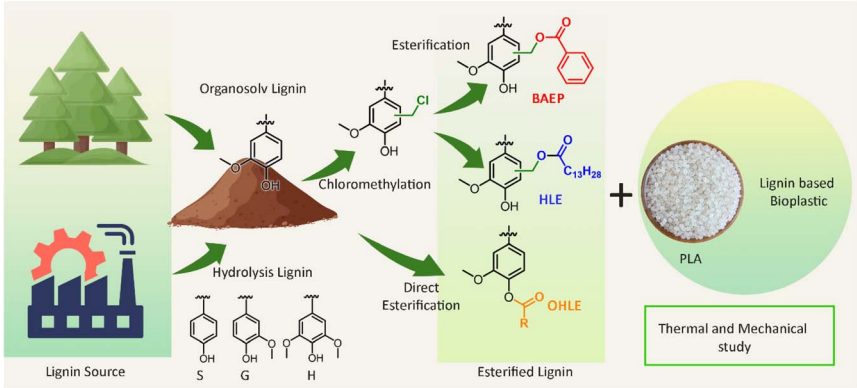

Fig. 1 Esterification of organosolv pine lignin and hydrolysis lignin in three different schemes and their compatibility study with PLA.

a conventional classification, softwood contains mostly guaiacyl units, and minor portions of *p*-hydroxyphenyl and syringyl; while, a hardwood's plant cell wall is predominantly composed of syringyl fragments, and a smaller quantity of guaiacyl; by contrast, all monolignols are present in non-woody biomass.[4,5] On an industrial scale, hydrolysis and organosolv pulping techniques are the two standard practices used to produce technical lignin. The former method focuses on using enzymatic treatment to liberate lignin from the recalcitrant biomass matrix, while the later employs aqueous organic solvents with or without a catalyst for the separation. The native lignin inevitably undergoes structural changes as a consequence of fractionation, which poses a challenge for its high-value-added applications.

Bio-derived polymers face several challenges, including poor interfacial adhesion with synthetic polymers, variations in purity due to differences in raw material sources, and complex extraction processes. These factors can hinder consistent material performance and limit broader applicability.[6] Lignin is a promising candidate for biocomposite production, due to its aromatic structure and high carbon content. The phenolic hydroxyl, carboxyl, and methoxy groups in lignin can be chemically modified to improve its compatibility with a variety of polymers. In recent decades, researchers have been focusing on potential application of lignin in various fields, including automotive components, bioplastics, adhesives, and antimicrobial packaging materials.[7–9] From a sustainability standpoint, lignin and its derivatives present a promising alternative to fossil-based plastics, helping to reduce reliance on petroleum-derived resources while promoting the development of bio-based materials.

Nevertheless, its structural complexity makes direct utilization challenging, which necessitates chemical modification to enhance its functionality and integration. Common modification strategies for lignin include depolymerization, the introduction of new reactive sites, and the functionalization of hydroxyl groups.[7] Techniques such as acetylation, esterification, and phenolation have been widely investigated.[8] Initial attempts to incorporate unmodified lignin into polypropylene often resulted in increased material stiffness but decreased tensile strength and elongation.[9] These drawbacks were primarily due to poor compatibility, specifically the weak adhesion between polar lignin and non-polar

Open Access Article. Published on 30 juin 2025. Downloaded on 11/04/2026 17:44:27. This article is licensed under a Creative Commons Attribution 3.0 Unported Licence.

polymers, which is attributed to strong self-interaction driven by inter- and intra-hydrogen bonding, causing lignin particles to agglomerate and act as stress concentrators within the composite.[10] Such limitations underscore the need for suitable chemical modifications to realize lignin's potential in polymer applications completely.[11,12] In contrast, acetylated lignin displays decreased hydrogen bonding because acetyl groups replace the hydroxyl groups during the acetylation. This modification makes acetylated lignin more hydrophobic and enhances its solubility in specific organic solvents.[13]

Esterification is the most frequently chosen pathway among different approaches to improve the thermoplasticity of lignin *via* chemical modification of hydroxy groups.[14] Those functional groups present as one of the significant active sites in lignin that can be functionalized with long-chain hydrocarbons, resulting in materials with improved thermoplasticity, flexibility of the polymer chain, hydrophobicity, and miscibility in nonpolar solvents as a consequence.[15] In a typical fashion, the synthesized material could be obtained by direct esterification with carboxylic acids,[16] acid anhydrides[17] or acid chlorides[18,19] in the presence of suitable catalysts. Recently, we have reported the development of a novel approach to esterify lignin *via* chloromethylation onto the aromatic rings at either the *ortho* or *meta*-position.[20] As an intermediate product, chloromethylated lignin (Fig. 1) offers highly reactive sites towards a variety of functionalization possibilities in which esterification using carboxylic acid is favourable. The obtained material has been successfully studied as a co-polymer blended with polylactic acid (PLA) for 3D printing purposes.[21]

In this work, we present a systematic comparison of two distinct esterification strategies for lignin modification: (i) direct esterification of hydroxyl groups using fatty acid chlorides, and (ii) a two-step process involving chloromethylation followed by reaction with carboxylic acids. The modified lignin samples were blended with polylactic acid (PLA) at varying ratios to assess compatibility and composite performance (Fig. 1). Additionally, the impact of hydrocarbon chain chemistry, such as saturated fatty acids and aromatic acids (*e.g.*, benzoic acid), on the physicochemical properties of the resulting lignin/PLA composites was examined. Two types of lignin were used: hydrolysis lignin from birch (a hardwood) and organosolv lignin from pine (a softwood) to highlight the broad potential of lignin for functionalization and application. The obtained materials were characterized using Fourier transform infrared spectroscopy (FT-IR), phosphorus nuclear magnetic resonance (^{31}P NMR), and 2D heteronuclear single quantum coherence (2D-HSQC). Additionally, the resulting biocomposites were characterized using differential scanning calorimetry (DSC), thermogravimetric analysis (TGA), and mechanical testing.

2. Materials and methods

2.1. Materials

PLA-Ingeo 3D850 from NatureWorks LLC-US, chloroform (99%), lauroyl chloride (98%), triethylamine, octanoyl chloride (99%), and palmitoyl chloride (98%) were purchased from Thermo Fischer Scientific. $CDCl_3$ and DMSO-d_6 from Eurisotop, as well as all reagents used, were of analytical reagent (AR) grade and were procured from Sigma-Aldrich (Taufkirchen, Germany). They were employed without further purification. Four distinct birch-derived hydrolysis lignin (HL)

Open Access Article. Published on 30 juin 2025. Downloaded on 11/04/2026 17:44:27. This article is licensed under a Creative Commons Attribution 3.0 Unported Licence.

samples were obtained from Fibenol OÜ (Estonia). The lignin was classified as hydrolysis lignin due to its production process, which involves enzymatic treatment. Longitudinally sawn pine timber sawdust was sourced from Prof. Jaan Kers (Tallinn University of Technology, Tallinn, Estonia).

The preparation of the biomass and organosolv lignin were carried out as described in an earlier study.[22]

2.2. Chloromethylation and esterification of lignin

The chloromethylation of organosolv lignin and hydrolysis lignin were carried out following our previously established procedure.[20] Esterification with benzoic acid was carried out by dissolving 2 g (1 eq.) of benzoic acid and 1.48 g (1 eq.) of K_2CO_3 in 20 mL of THF. The reaction mixture was heated to 70 °C and was maintained at this temperature for 1 hour. Subsequently, 66 mg of KI and 2 g of chloromethylated lignin (previously dissolved in 30 mL of THF) was added. The mixture was then refluxed overnight. After the reaction was completed, the mixture was cooled to room temperature, and the solvent was removed under reduced pressure. The residue was extracted using an ethyl acetate–water system. The organic layer was washed successively with a saturated $NaHCO_3$ solution, water, and brine, then dried over anhydrous Na_2SO_4. Finally, the solvent was removed under reduced pressure, and the product was precipitated in hexane. Esterification of the hydrolysis lignin with tetradecanoic acid was carried out following our previously published procedure.[21]

2.3. Chlorine content *via* XRF analysis

X-ray fluorescence (XRF) spectroscopy was used for the determination of chlorine content in chloromethylated lignin. Quantitation was performed using a Bruker S4 PIONEER wavelength-dispersive XRF spectrometer using an Rh anode under vacuum. Lignin samples were pressed into pellets to ensure homogeneity. Chlorine analysis was performed with a PET crystal and with Bruker's pre-calibrated methodology. The theoretical maximum chlorine content of 15.4 wt% was computed from the chloromethylated guaiacyl (G) unit (229.45 g mol^{-1}) to facilitate the evaluation of the efficiency of chloromethylation *via* mass-to-mass comparison with the XRF data.

2.4. Lignin–OH groups esterification

The direct esterification of organosolv lignin, *via* its hydroxyl groups, was prepared as reported.[23] 1 g of lignin was weighed and dissolved in a 100 mL round-bottom flask containing 10 mL of dry THF. Later, 300 μL of triethylamine (TEA, 1.5 eq. to total OH groups, 2.87 mmol g^{-1} of lignin[22]) was added and mixed for 10 minutes. The mixture was then kept in an ice bath for 10 minutes, and fatty acid chlorides (367 μL of octanoyl-C8, 506 μL of lauroyl-C12, or 657 μL of palmitoyl-C16 chlorides) (1.5 equivalents to the total OH groups) were added.[22] The reaction was carried out at room temperature for 4 hours, under vigorous stirring. Upon completion, 50 mL of chloroform was added, and the mixture was transferred to a separatory funnel for liquid–liquid extraction using 30 mL of a 5% sodium hydroxide solution. The organic layer was gathered, and the solvent was evaporated to collect the modified lignin. The final materials were washed three times with 50 mL of 100% ethanol to remove unwanted by-products. The esterified lignin samples were freeze-dried to remove all solvent residue.

Open Access Article. Published on 30 juin 2025. Downloaded on 11/04/2026 17:44:27. This article is licensed under a Creative Commons Attribution 3.0 Unported Licence.

2.5. PLA/lignin film preparation

PLA was separately dissolved in DCM in a 15 mL glass vial. Lignin was dissolved in THF at room temperature and then mixed to achieve a lignin content of 10% to 30% w/w. Our previous study[21] showed that at 40% lignin esters with PLA, a reduction in T_g was observed. Based on these results, we have considered only up to 30% as the maximum in this work. The dissolved components were combined in a Petri dish and allowed to dry overnight. After the initial drying phase, the composite material underwent further drying in a vacuum oven at 40 °C for an additional 12 hours.

2.6. Fourier transform infrared spectroscopy (FT-IR)

The infrared spectra of the lignins were recorded by IRTracer-100 (Shimadzu, Japan). The measurements were conducted in two modes: diffuse reflection and attenuated total reflection (ATR). All spectra were recorded in the range of 4000–400 cm^{-1} for 80 scans.

2.7. Nuclear magnetic resonance (NMR)

NMR analysis was measured as ^{31}P for determination of the hydroxyl contents and 2D-heteronuclear single quantum coherence (2D-HSQC) for structural characterization. For the ^{31}P experiment, approximately 30 mg of lignin was dissolved in 500 μL of pyridine and $CDCl_3$ (1.6 : 1 v/v). Upon solubilization, 100 μL of the internal standard (*N*-hydroxy-5-norbornene-2,3-dicarboximide, 20 mg mL^{-1}) and 100 μL of relaxation agent (chromium(III) acetyl-acetonate, 5 mg mL^{-1}), which were prepared in the same mixture of pyridine and chloroform, were added to the vial containing the solubilized lignin. Finally, 70 μL of 2-chloro-4,4,5,5-tetramethyl-1,3,2-dioxaphospholane, and a phosphorus derivatization reagent, were added. ^{31}P data were acquired at 25 °C using an inverse gated decoupling pulse sequence (zgig), with 1500 scans, on a Bruker Avance III 400 MHz spectrometer. Data acquisition for 2D-HSQC was carried out on the hydrolyzed lignin and its derivatives. 40 mg of the samples were dissolved in 600 μL of DMSO-d_6. Experimental data were achieved using a Bruker Avance III 800 MHz spectrometer with hsqcetgpsisp2.2 pulse sequence, four scans. Data analysis was assisted by the MestReNova software.

2.8. Differential scanning calorimetry

Differential scanning calorimetry (DSC) was performed using a PerkinElmer DSC 6000 calorimeter with an IntraCooler II as the cooling system at a constant heating rate of 10 °C min^{-1} in a pure nitrogen atmosphere (purity 99.999%, purge at 20 mL min^{-1}). A sample mass of 5 mg ± 2 mg was used for all materials. Samples were pressed into the aluminium crucible using the aluminium lid to improve contact between the material and the crucible.

2.9. Thermogravimetry

Thermogravimetric analysis (TGA) was performed using a NETZSCH STA 449 F3 Jupiter® apparatus. The samples were heated in a pure nitrogen atmosphere (purity 99.999%, purge at 40 mL min^{-1}) from 25 °C to 400 °C at a constant heating

rate of 10 °C min^{-1}. The mass of the samples was 4.8 ± 0.9 mg. Aluminium crucibles were used.

2.10. Mechanical testing

Biocomposites were tested mechanically using an Instron 5866 instrument (ASTM D638 standard) (Instron, US) and a load cell of 2.5 kN (force sensor capable of measuring up to 2.5 kN of force). A grip distance of 30 mm was used for a 10 mm wide film.

3. Results and discussion

3.1. Characterization of lignin and its modification

We previously demonstrated the esterification followed by chloromethylation of pine lignin, and the same methodology was applied to hydrolysis lignin. NMR proved the chloromethylation procedure to be as efficient for in-house lignin as it was for *in situ* extracted pine lignin. In the ^{1}H NMR spectra, the characteristic peak at 4.5–4.75 ppm (Fig. S1 and S2†) confirms the presence of CH_2–Cl. For further confirmation, 2D-HSQC measurement with a higher order in dimension that offers a deeper understanding of lignin structure (*e.g.*, inter-unit linkages, and subunits) was analysed for the hydrolysis of birch lignin.[24,25] As a rule of thumb for the 2D-HSQC interpretation of lignin, focused on two major informative areas: (i) the oxygenated aliphatic side chain (C/H 100–35/6–2.5 ppm), (ii) aromatic or unsaturated carbon (C/H 150–100/8.0–6.0 ppm). All the spectra were calibrated at the solvent signal of DMSO-d_6 (C/H 39.51/2.50 ppm). As a result, the new reactive groups were successfully introduced onto aromatic rings in lignin, as verified by two distinct cross-peaks appearing at C/H 37.97/4.8 and 40.61/4.63 ppm, marked as an asterisk in Fig. 2c, compared to those of the starting material (Fig. 2a). Since the introduction of new functional groups could occur at either the *ortho* or *meta*-position, it explains the emergence of two distinguishable signals in the HSQC spectra. This observation was consistent with the previous ^{1}H NMR data. Methoxy is one of the most abundant functional groups in lignin, which supply the intense and stable cross signal at C/H 55.62/3.77 ppm before and after chemical modification, however, the ether linkage (β-O-4′) peaks ($A_{\beta(S)}$: C/H 86.06/4.11) undergo substantial decrease in chloromethylation-modified lignin. This can be explained by the fact that the acidic media used in the chloromethylation step depolymerized lignin into smaller fragments by breaking down the labile bond, as also evidenced in our previous study.[20] Moving to the aromatic area of the HSQC spectra, they were strongly indicated by the cross signals of the S and G units as two main monolignols in the hardwood species at C/H 104.30/6.60 and 118.5–110.11/6.90–6.76 ppm, respectively[26] (Fig. 2b). After chloromethylation (Fig. 2d), the intensity of all these peaks drastically declines, confirming that the substitution occurred on the aromatic rings, as per our hypothesis. It is worth noting that, despite the higher degree of methoxylation in S than G units, steric hindrance was not a barrier for introducing new functional groups onto other positions on S-rings.

On the other hand, a ^{31}P NMR measurement was employed to investigate the impact of the esterification process on the –OH groups through the two pathways: using acid chlorides targeting hydroxy groups, and chloromethylation followed by

Open Access Article. Published on 30 juin 2025. Downloaded on 11/04/2026 17:44:27. This article is licensed under a Creative Commons Attribution 3.0 Unported Licence.

Open Access Article. Published on 30 juin 2025. Downloaded on 11/04/2026 17:44:27.
This article is licensed under a Creative Commons Attribution 3.0 Unported Licence.

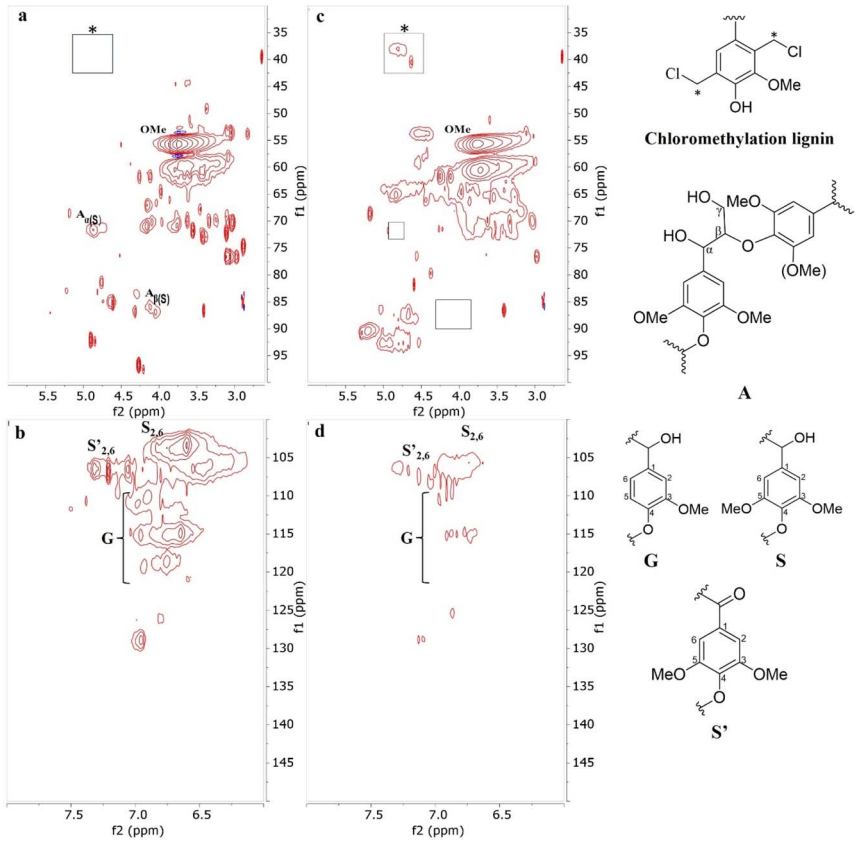

Fig. 2 2D-HSQC of hydrolysis lignin (a and b), chloromethylation lignin (c and d). Two regions of investigation: oxygenated aliphatic side chain (C/H 100–35/6.0–2.5 ppm) (top), aromatic/unsaturated region (C/H 150–100/8.0–6.0 ppm) (bottom). The lignin's subunits are shown on the right side.

esterification. All the spectra were referenced at the internal standard signal of 151.8 ppm before analysis. As a softwood species, phenolic hydroxy groups were predominantly found for G and H units (Fig. S3a†).[27] These functional groups were expected to be consumed in the direct esterification approach, as shown in Fig. S3b,† which shows a significant decrease. At the same time, aliphatic hydroxyl groups show a slight change. In the chloromethylated sample (Fig. S3c†), there is a profound shift of the origin of OH groups from G units towards the regions of condensed OH (from around 139.0 to 144.0 ppm). Still, it does not disappear, as observed in the first case. The shifting can be explained by two facts: (i) the attachment of chloromethyl to aromatic rings of lignin mimic a similar structure of condensed lignin, (ii) the electronegativity of chloride atoms contributes to the decrease of electron density on the aromatic rings, which causes the shifting towards lower field or higher chemical shift. Later, the grafting of benzoic acid was confirmed by the shift of the signal at approximately 144.0 ppm to a lower chemical shift of 142.4 ppm (Fig. S3d†), indicating that the electronegative groups

Open Access Article. Published on 30 juin 2025. Downloaded on 11/04/2026 17:44:27.
This article is licensed under a Creative Commons Attribution 3.0 Unported Licence.

were replaced successfully, resulting in a balance in electron density due to the attachment of a conjugation system.

XRF analysis further confirms that 13.3% and 13.6% of chlorine is present in the chloromethylated hydrolysis lignin and organosolv pine lignin, respectively. The esterification reaction was confirmed through ^{1}H NMR. A comparison study revealed the disappearance of the chloromethylated peak (ph–CH_2–Cl) and the emergence of a new peak (ph–CH_2–O), corresponding to the methylene moieties, indicating the formation of the ester (HLE) (Fig. S1†).

The esterification of hydrolysis lignin with tetradecanoic acid (HLE) was confirmed by the enhanced intensity of the two bands around 2918 and 2846 cm^{-1}, which are attributed to CH_2 stretching vibrations in the methyl and methylene groups of the ester side chains (Fig. 3a). Additionally, a slightly merged absorption band at 1734 cm^{-1} corresponds to C=O stretching vibrations, while the band at 1575 cm^{-1} and 1541 cm^{-1} is associated with aromatic skeletal vibrations in lignin, as shown in Fig. 3a. The complex and heterogeneous structure of lignin, with aromatic moieties, makes it challenging to differentiate between peaks arising from native lignin and those introduced through esterification with benzoic acid. The absorption bands arising at 1740 cm^{-1} and 1464 cm^{-1} correspond to the ester C=O and aromatic stretching vibrations. The C–H deformation vibration absorption at 713 cm^{-1}, typical of monosubstituted benzene compounds, will confirm the benzoic acid ester (BAEP) in Fig. 3b.

For all the direct esterification samples using fatty acid chlorides (C8, C12, C16) (Fig. 3c), the successful modification was confirmed by the appearance of two characteristic signals at 1740 cm^{-1} and 1760 cm^{-1} representing aliphatic and

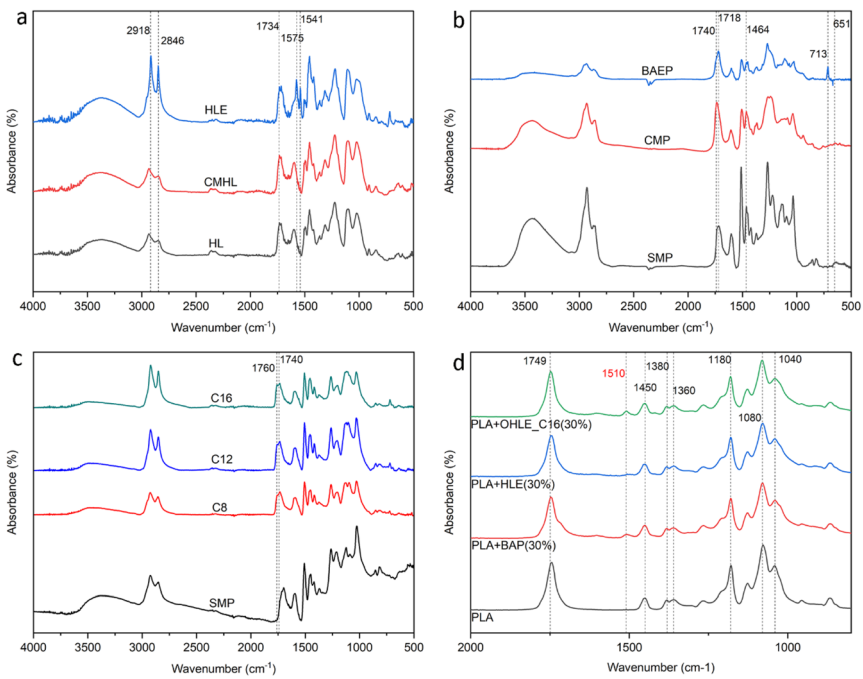

Fig. 3 FT-IR measurements for hydrolysis lignin esters (HLE) (a), lignin benzoic acid ester (BAEP) (b), direct esterified lignin (OHLE) derivatives (c), and PLA/lignin ester films (d).

Open Access Article. Published on 30 juin 2025. Downloaded on 11/04/2026 17:44:27. This article is licensed under a Creative Commons Attribution 3.0 Unported Licence.

aromatic esters, respectively.[28] Moreover, the OH stretching vibration band at 3440 cm^{-1} experienced an incremental decline, which further verifies the consumption of hydroxy groups during the esterification. The variation in attached hydrocarbon chain length (from C8 to C16) was observed as a slight increase within the region of aliphatic C–H stretching 2918–2846 cm^{-1}. The work-up procedure was proven to be efficient as the absence of a carbonyl chloride (Cl–C═O) signal at 1800 cm^{-1}, which originates from unreacted acid chloride,[29] indicated that no side products were detected.

The FT-IR spectra of PLA/lignin composites showed the characteristic band of neat PLA (Fig. 3d). The prominent peak at 1749 cm^{-1} is attributed to C═O stretching vibrations, and that at 1450 cm^{-1} is due to antisymmetric bending of CH_3 groups. Peaks associated with deformation and bending vibrations of CH groups appear at 1380 cm^{-1} and 1360 cm^{-1}. C–O–C stretching vibrations are present at 1180, 1080, and 1040 cm^{-1}. A weak band at 1510 cm^{-1} for C═C stretching of an aromatic ring was observed in the biocomposites with lignin.

3.2. Thermal behaviour: DSC, TG, and DTG of esterified lignin/PLA composite

The thermal properties of PLA can be systematically altered by incorporating modified lignin at different loadings. Our previous study explored changes in T_g of PLA loaded with organosolv pine lignin modified with fatty acids. Lignin tetradecanoic acid (C14) at 30% was found to provide the maximum improvement in the glass transition temperature.[21] Similarly, PLA with hydrolysis lignin esters (HLE) resulted in a gradual increase in the glass transition temperature (T_g) from 66 °C to 70 °C, as the concentration increases from 10% to 30%, while reducing C_p values, indicating enhanced thermal stability of the glassy phase and flexibility of the polymer matrix (Fig. 4a). In contrast, phenolic-OH esterified lignin (OHLE) mixed with PLA exhibited various trends depending on the alkyl chain length. OHLE_C8 and OHLE_C12 showed T_g values close to PLA but moderately increased ΔC_p, suggesting balanced flexibility. Remarkably, OHLE_C16 reduces both T_g (down to 55 °C) and ΔC_p, as shown in Fig. 4b, indicating a strong plasticization effect. Benzoic acid ester lignin (BAEP) with PLA exhibited an increase in T_g, reaching 70 °C at a 30% loading, accompanied by a moderately rising ΔC_p, indicating improved thermal properties at higher concentrations. Thus, the results of the present study suggest that HLE-30%, OHLE_C16-30%, and BAEP-30% should be chosen for further studies.

The thermogravimetric (TG) data (Fig. 4c) reveal the thermal stability of the PLA/lignin esters. All samples show a gradual decrease in mass with increasing temperature. Mass loss occurs in two separate temperature ranges, initiating at around 80 °C and again at approximately 245 °C. The mass loss observed at 80 °C is due to the evaporation of humidity and chemically bound water. Significant thermal decomposition begins at 245 °C, marking the onset of substantial degradation, with the degradation rate increasing with the temperature rise. Among them, PLA, BAP-30%, and HLE-30% exhibit a similar trend of degradation, while the OHLE_C16-30% sample shows the lowest thermal stability. However, BAP-30% shows a slightly higher mass loss at temperatures preceding thermal degradation onset. The differential thermogravimetric (DTG) analysis (Fig. 4d) reveals the differences in thermal degradation behavior. BAP-30% exhibits slightly higher DTG values at the intermediate temperature range of 80 °C

Open Access Article. Published on 30 juin 2025. Downloaded on 11/04/2026 17:44:27.
This article is licensed under a Creative Commons Attribution 3.0 Unported Licence.

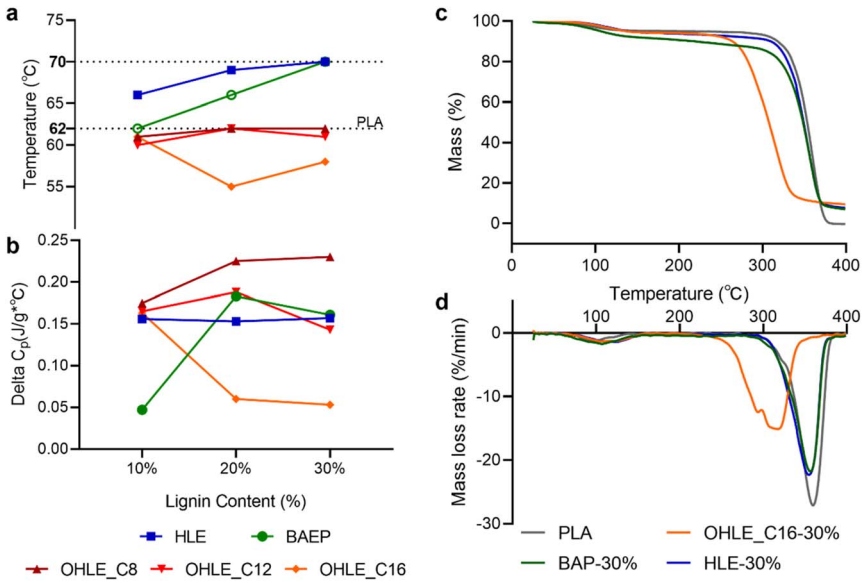

Fig. 4 Glass transition temperature (a), delta C_p (b), thermogravimetric (c), and differential thermogravimetric (d) studies for PLA/lignin film.

to 120 °C. OHLE_C16-30% exhibits an early degradation trend, whereas HLE-30% and BAP-30% display similar DTG trends to PLA. These results suggest that the OHLE_C16-30% is the least thermally stable, due to the lack of phenolic hydroxyl groups to form hydrogen bonds. In contrast, esterification through chloromethylation provides the free hydroxyl groups, which are likely to have stronger intermolecular interactions and result in a more thermally stable structure.

Overall, compared to the thermal properties of common fossil-based plastics like polyethylene terephthalate (PET, T_g 70–87 °C),[30] all esterified lignin/PLA composites show slightly lower glass transition temperatures (T_g 55–70 °C). The same applies to the selected loading at 30% of modified lignin (OHLE C16, BAP, and HLE) with PLA (T_g 58–70 °C).

3.3. Mechanical properties

Based on the DSC properties, neat PLA and its composites with 30 wt% lignin esters (HLE, OHLE_C16, and BAEP) were examined for tensile properties, and are listed in Fig. 5 and Table S1.† The neat PLA film exhibited the maximum load (15.2 ± 2 N) (Fig. 5a), indicating greater load-carrying capacity compared to other modified composites. Significantly, the PLA + HLE (30%) composite showed reduced maximum load (8.5 ± 2 N) yet the highest tensile stress among all other modified composites (Fig. 5b), which shows improvement in the strength of the material in terms of cross-sectional area after the addition of HLE. In contrast, PLA + OHLE_C16 (30%) and PLA + BAEP (30%) composites exhibited lower maximum loads and tensile stresses, with PLA + BAEP (30%) recording the lowest tensile stress, indicating a loss of strength.

Tensile extension to the maximum increased upon lignin ester addition (Fig. 5c), showing enhanced ductility of the composite materials. Maximum

Open Access Article. Published on 30 juin 2025. Downloaded on 11/04/2026 17:44:27.
This article is licensed under a Creative Commons Attribution 3.0 Unported Licence.

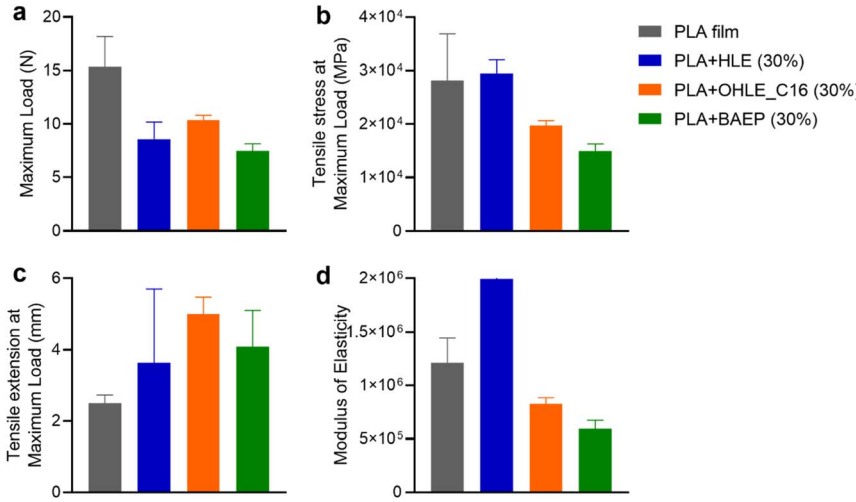

Fig. 5 (a) Maximum load, (b) tensile stress at maximum load, (c) tensile extension at maximum load, (d) Young's modulus of PLA/lignin film.

elongation was observed for PLA + OHLE_C16 (30%), followed by PLA + HLE and PLA + BAEP, while neat PLA had the minimum extension. This shows that the addition of lignin esters reduces the brittleness of the PLA matrix and enhances its flexibility. The most structurally similar commercial plastic derived from fossil fuel resources, polystyrene (PS), has tensile strength ranging from 35 to 51 MPa,[30] which is lower than PLA itself. This transitive comparison proves that the composite consists of PLA and 30% HLE is a promising material to replace fossil-based plastic.

The modulus of elasticity (Fig. 5d), being a measure of material stiffness, was greatly influenced by the form of lignin ester used. PLA + HLE (30%), followed by neat PLA, possessed the largest modulus, thereby indicating increased stiffness by incorporating HLE. Both the other composites, namely PLA + OHLE_C16 (30%) and PLA + BAEP (30%), exhibit a lower modulus, indicating a softening effect on the PLA matrix.

In conclusion, the mechanical characteristics of PLA composites depend to a great extent on the nature of the incorporated lignin ester. Among the under-examined samples, PLA + HLE (30%) exhibited higher tensile stress and stiffness, and is therefore most suitable for applications requiring enhanced mechanical strength and rigidity. PLA + OHLE_C16 (30%) improved ductility at the expense of strength and stiffness, making it ideal for more elastic applications. PLA + BAEP (30%) possessed the worst mechanical properties, suggesting minimal structural reinforcement. This result demonstrates the tunability of the mechanical properties of PLA through lignin ester modification and the potential of HLE as an effective reinforcing agent.

4. Conclusions

Lignin isolated by two different processes – organosolv and hydrolysis – were chemically modified through direct esterification at the hydroxyl groups and

esterification *via* chloromethylation. The resulting lignin esters were subsequently characterized and incorporated into PLA at varying concentrations (10%, 20%, and 30%) using the solvent casting technique. Thermal and mechanical analysis of the blended composites revealed that the introduction of ester moieties into lignin affects the thermal and mechanical behaviour of the polymer matrix. Notably, PLA was able to accommodate up to 30% of lignin esters. Among the modifications, HLE and BAEP modifications improve the thermal characteristics of PLA, whereas OHLE_C16 provides enhanced flexibility through plasticization. These results underscore that the overall characteristics of PLA composites strongly depend on the type of lignin ester introduced. The results demonstrate the potential for tailoring the thermal and mechanical properties of PLA through selective lignin esterification approaches, offering a promising avenue for the production of high-performance, sustainable bioplastics.

Data availability

The following data associated with this work can be found in the ESI.† ^{1}H NMR spectra of hydrolysis lignin (HL), chloromethylated hydrolysis lignin (CMHL), and hydrolysis lignin esters (HLE) (Fig. S1†); ^{1}H NMR spectra of organosolv pine lignin (OPL), chloromethylated pine lignin (CMPL), and benzoic acid ester pine (BAEP) (Fig. S2†); ^{31}P NMR spectra of organosolv pine lignin (a), C16 ester modified OH of pine lignin (b), chloromethylated pine lignin (c), and benzoic acid ester pine (d) (Fig. S3†); the tensile properties of neat PLA and its composites with 30 wt% lignin esters (HLE, OHLE_C16, and BAEP) (Table S1†).

Author contributions

The manuscript was written through the contributions of all authors. All authors have approved the final version of the manuscript. Mahendra K. Mohan: conceptualization; methodology; investigation – organosolv extraction, chemical modification, characterization, thermal and mechanical testing; validation; data curation; visualization; writing – original draft preparation. Tran Ho: methodology; investigation – organosolv lignin extraction, esterification, characterisation, NMR analysis; validation; data curation; writing – original draft preparation. Carmen Köster: investigation – technical lignin characterisation and modification; validation; data curation; writing – original draft preparation. Oliver Järvik: investigation – thermal analysis; validation; data curation; writing – reviewing and editing. Maria Kulp: methodology, writing – reviewing and editing. Yevgen Karpichev: conceptualization, methodology; resources; funding acquisition; writing – reviewing and editing; project administration.

Conflicts of interest

The authors declare that they have no known competing financial interests or personal relationships that could have appeared to influence the work reported in this paper.

Open Access Article. Published on 30 juin 2025. Downloaded on 11/04/2026 17:44:27. This article is licensed under a Creative Commons Attribution 3.0 Unported Licence.

Open Access Article. Published on 30 juin 2025. Downloaded on 11/04/2026 17:44:27. This article is licensed under a Creative Commons Attribution 3.0 Unported Licence.

Acknowledgements

The Estonian Research Council supported this work *via* project TEM-TA49. The valuable technical support of Dr Illia Krasnou, Dr Marina Kudrjašova, and Dr Indrek Reile is gratefully acknowledged. The authors acknowledge Muhammad Afaq Khan for organosolv lignin extraction.

References

1 R. Shorey, A. Salaghi, P. Fatehi and T. H. Mekonnen, *RSC Sustainability*, 2024, **2**, 804–831.
2 J. Ralph, C. Lapierre and W. Boerjan, *Curr. Opin. Biotechnol.*, 2019, **56**, 240–249.
3 S. Sethupathy, G. Murillo Morales, L. Gao, H. Wang, B. Yang, J. Jiang, J. Sun and D. Zhu, *Bioresour. Technol.*, 2022, **347**, 126696.
4 V. K. Ponnusamy, D. D. Nguyen, J. Dharmaraja, S. Shobana, J. R. Banu, R. G. Saratale, S. W. Chang and G. Kumar, *Bioresour. Technol.*, 2019, **271**, 462–472.
5 A. V. Faleva, A. Yu. Kozhevnikov, S. A. Pokryshkin, D. I. Falev, S. L. Shestakov and J. A. Popova, *J. Wood Chem. Technol.*, 2020, **40**, 178–189.
6 J. Sameni, S. A. Jaffer and M. Sain, *Composites, Part A*, 2018, **115**, 104–111.
7 P. Figueiredo, K. Lintinen, J. T. Hirvonen, M. A. Kostiainen and H. A. Santos, *Prog. Mater. Sci.*, 2018, **93**, 233–269.
8 F. Taleb, M. Ammar, M. ben Mosbah, R. ben Salem and Y. Moussaoui, *Sci. Rep.*, 2020, **10**, 11048.
9 R. Pucciariello, V. Villani, C. Bonini, M. D'Auria and T. Vetere, *Polymer*, 2004, **45**, 4159–4169.
10 D. Kun and B. Pukánszky, *Eur. Polym. J.*, 2017, **93**, 618–641.
11 C. Wang, S. S. Kelley and R. A. Venditti, *ChemSusChem*, 2016, **9**, 770–783.
12 E. A. Agustiany, M. Rasyidur Ridho, M. Rahmi D. N., E. W. Madyaratri, F. Falah, M. A. R. Lubis, N. N. Solihat, F. A. Syamani, P. Karungamye, A. Sohail, D. S. Nawawi, A. H. Prianto, A. H. Iswanto, M. Ghozali, W. K. Restu, I. Juliana, P. Antov, L. Kristak, W. Fatriasari and A. Fudholi, *Polym. Compos.*, 2022, **43**, 4848–4865.
13 U. Hwang, B. Lee, B. Oh, H. S. Shin, S. S. Lee, S. G. Kang, D. Kim, J. Park, S. Shin, J. Suhr, S.-H. Kim and J.-D. Nam, *Eur. Polym. J.*, 2022, **165**, 110971.
14 S. Laurichesse and L. Avérous, *Prog. Polym. Sci.*, 2014, **39**, 1266–1290.
15 A. Lisý, A. Ház, R. Nadányi, M. Jablonský and I. Šurina, *Energies*, 2022, **15**, 6213.
16 P. Hafezisefat, L. Qi and R. C. Brown, *ACS Sustain. Chem. Eng.*, 2023, **11**, 17053–17060.
17 S. N. Pawar, R. A. Venditti, H. Jameel, H.-M. Chang and A. Ayoub, *Ind. Crops Prod.*, 2016, **89**, 128–134.
18 O. Gordobil, E. Robles, I. Egüés and J. Labidi, *RSC Adv.*, 2016, **6**, 86909–86917.
19 O. Gordobil, I. Egüés and J. Labidi, *React. Funct. Polym.*, 2016, **104**, 45–52.
20 M. K. Mohan, O. Silenko, I. Krasnou, O. Volobujeva, M. Kulp, M. Ošeka, T. Lukk and Y. Karpichev, *ChemSusChem*, 2024, **17**, e202301588.
21 M. K. Mohan, I. Krasnou, T. Lukk and Y. Karpichev, *ACS Omega*, 2024, **9**, 44559–44567.
22 P. Jõul, T. T. Ho, U. Kallavus, A. Konist, K. Leiman, O.-S. Salm, M. Kulp, M. Koel and T. Lukk, *Materials*, 2022, **15**, 2861.

23 E.-L. Hult, J. Ropponen, K. Poppius-Levlin, T. Ohra-Aho and T. Tamminen, *Ind. Crops Prod.*, 2013, **50**, 694–700.
24 J.-L. Wen, S.-L. Sun, B.-L. Xue and R.-C. Sun, *Materials*, 2013, **6**, 359–391.
25 T.-Q. Yuan, S.-N. Sun, F. Xu and R.-C. Sun, *J. Agric. Food Chem.*, 2011, **59**, 10604–10614.
26 Z. Wang and P. J. Deuss, *ChemSusChem*, 2021, **14**, 5186–5198.
27 L. Lagerquist, A. Pranovich, I. Sumerskii, S. von Schoultz, L. Vähäsalo, S. Willför and P. Eklund, *Molecules*, 2019, **24**, 335.
28 K. A. Y. Koivu, H. Sadeghifar, P. A. Nousiainen, D. S. Argyropoulos and J. Sipilä, *ACS Sustain. Chem. Eng.*, 2016, **4**, 5238–5247.
29 R. Shorey and T. H. Mekonnen, *Int. J. Biol. Macromol.*, 2023, **230**, 123143.
30 F. Luzi, L. Torre, J. M. Kenny and D. Puglia, *Materials*, 2019, **12**, 471.

Open Access Article. Published on 30 juin 2025. Downloaded on 11/04/2026 17:44:27.
This article is licensed under a Creative Commons Attribution 3.0 Unported Licence.